Palaeogeography, Palaeoclimatology, Palaeoecology xxx (xxxx) xxxx

Contents lists available at ScienceDirect

Palaeogeography, Palaeoclimatology, Palaeoecology

journal homepage: www.elsevier.com/locate/palaeo

Vegetation change in the Baringo Basin, East Africa across the onset of Northern Hemisphere glaciation 3.3–2.6 Ma

Rachel L. Lupien[a,b,*], James M. Russell[a], Chad L. Yost[c], John D. Kingston[d], Alan L. Deino[e], Jon Logan[c], Anna Schuh[c], Andrew S. Cohen[c]

[a] Brown University, Department of Earth, Environmental, and Planetary Sciences, 324 Brooke Street, Providence, RI, 02906, USA
[b] Lamont-Doherty Earth Observatory, Division of Biology and Paleo Environment, 61 Route 9W, Palisades, NY, 10964, USA
[c] University of Arizona, Department of Geosciences, 1040 East 4th Street, Tucson, AZ, 85721, USA
[d] University of Michigan, Department of Anthropology, 1085 South University Avenue, Ann Arbor, MI, 48109, USA
[e] Berkeley Geochronology Center, 2455 Ridge Road, Berkeley, CA, 94709, USA

ARTICLE INFO

Keywords:
Paleoclimatology
Pliocene
Organic geochemistry
Leaf waxes
Carbon isotopes
Human evolution

ABSTRACT

Vegetation in East Africa is generally thought to have shifted from forests to more open grasslands and savannas as global climate cooled and high-latitude ice sheets expanded during the Plio-Pleistocene. Such a shift would have greatly influenced landscape resources, and potentially hominin evolution as well. Existing records of African vegetation spanning these time-scales are generally derived from offshore marine records that record continental-scale changes, or paleosol carbonate records that record very local vegetation changes during the short time intervals of soil carbonate formation. Here we present a new record of basin-scale vegetation change from the late Pliocene (~3.3–2.6 Ma) derived from a drill core from the Chemeron Formation, located in the Baringo Basin/Tugen Hills region of the Kenya Rift Valley. Specifically, we present a new record of the relative abundance of C_4 grasses and C_3 vegetation based on the carbon isotopic composition of leaf wax biomarkers ($\delta^{13}C_{wax}$), which captures a signal of regional vegetation change. These data demonstrate that vegetation in the Baringo Basin varied greatly between C_3 forests and C_4 grasslands, and that vegetation exhibits both long-term (secular) trends and orbital-scale variations. The contribution of C_3 plants was lower than estimates based on low-resolution carbon isotope data from paleosol carbonates and organic matter in the basin. C_3 plants averaged ~53% of the vegetation during the late Pliocene, from ~3.3 to ~3.04 Ma, after which time $\delta^{13}C_{wax}$ indicates more open vegetation and ~41% C_3 plants. This transition may have been driven by changes in basin geomorphology, but also possibly occurred as part of larger-scale drying and expansion of C_4 vegetation in East Africa. In addition to this secular change, we observe high amplitude variability in the $\delta^{13}C_{wax}$ record including oscillations between ~80 and ~0% C_3 plants. These vegetation changes are correlated with changes in precipitation inferred from δ^2H_{wax} and lake level oscillations inferred from sedimentary facies, implying that high-amplitude, orbital-scale variations in precipitation drove significant changes in vegetation resources during the late Pliocene in the Baringo Basin. These variations have important implications for changes in terrestrial resources in light of the evolutionary innovations in the hominin fossil record related to changes in foraging strategies.

1. Introduction

Understanding the mechanisms linking hominin and mammalian evolution to past climate change is an enduring challenge. Vegetation provides critical nutrition, shelter, and other ecosystem services, and is thus perhaps the most critical environmental variable linking climate to human ecologies. It has been repeatedly suggested that hominin turnover, dispersal, and new technologies coincide with changes in climate and vegetation (Vrba, 1985; e.g. Potts and Faith, 2015); however, the precise spatiotemporal characteristics of changes in rainfall, vegetation, East African landscapes, and hominin evolution are still poorly constrained, allowing for a range of hypotheses about the processes driving hominin evolution (Kingston et al., 2007). Paleobotanical records indicate gradual expansion of C_4 grasslands starting in the late Miocene and continuing through the Pliocene and Pleistocene in East Africa (Cerling and Hay, 1986; Cerling, 1992; Bobe et al., 2002; Bobe and Behrensmeyer, 2004; Bonnefille, 2010; Levin et al., 2011; Uno et al., 2016a; Polissar et al., 2019). Multiple datasets (deMenocal, 2004;

* Corresponding author. Lamont-Doherty Earth Observatory, Division of Biology and Paleo Environment, 61 Route 9W, Palisades, NY, 10964, USA.
E-mail address: rlupien@ldeo.columbia.edu (R.L. Lupien).

https://doi.org/10.1016/j.palaeo.2019.109426
Received 3 February 2019; Received in revised form 21 October 2019; Accepted 24 October 2019

Campisano and Feibel, 2007; Maslin and Christensen, 2007; Trauth et al., 2007, 2010; Maslin and Trauth, 2009; Lupien et al., 2018) and hominin evolutionary modelling studies (e.g. Grove, 2014, 2015) have also explored variability in the amplitude of East African climate and vegetation at orbital time-scales (10^4 years) and their potential links to human evolutionary change (Potts, 1996, 1998). Despite these advances, we still lack high-resolution paleoenvironmental records from most of the basins in which hominin fossils are found, limiting our ability to test paleoanthropological hypotheses.

The most comprehensive evidence for the long-term expansion of C_4 grasslands in East Africa is from pedogenic carbonate carbon isotope ($\delta^{13}C_{SC}$) records. Levin (2015) compiled datasets from numerous East African sedimentary basins and documented trends towards less negative $\delta^{13}C_{SC}$ values, taken to indicate more open, C_4-dominated ecosystems over the past 10 million years. This C_4 expansion has often been interpreted to reflect large-scale changes in Plio-Pleistocene climate, and in particular gradual drying in East Africa linked to global cooling (deMenocal, 1995, 2004; Cerling et al., 1997; Maslin et al., 2014; Uno et al., 2016a). However, the amplitude and timing of shifts in the $\delta^{13}C_{SC}$ records vary considerably by basin, perhaps suggesting a series of vegetation changes driven by more local environmental conditions (Levin, 2015). Soil carbonates also record vegetation type only during time intervals and sites of soil carbonate production, i.e. soil types during warmer seasons and phases of orbital-scale climate cycles causing semi-arid conditions (Breecker et al., 2009; Cerling et al., 2011), and thus may not constrain the full range of vegetation changes occurring across basins and through time. Marine records of terrestrial vegetation derived from fossil pollen and leaf wax carbon isotope data ($\delta^{13}C_{wax}$) are consistent with inferences from $\delta^{13}C_{SC}$ (Feakins et al., 2005, 2013), although some records also suggest minimal change in vegetation during the Plio-Pleistocene (Rose et al., 2016). Moreover, the marine records generally lack the continuity and temporal resolution to determine the timing and magnitude of vegetation changes. These limitations hamper our ability to evaluate the linkages between long-term, global climate change, East African climates and vegetation, and human evolution.

Even fewer records provide an opportunity to evaluate variability in vegetation at orbital to sub-orbital timescales. This stands in contrast to records of East African paleohydrology, where there are now records from lake levels, marine sedimentation, isotopic composition of meteoric waters, and other proxies that document variability in water resources and their links to orbital forcing (e.g. Rossignol-Strick, 1983; Deino et al., 2006; Kingston et al., 2007; Joordens et al., 2011; Tierney et al., 2017; Lupien et al., 2018). Although we still lack continuous orbitally resolved records of continental paleohydrology spanning the Plio-Pleistocene, the existing records generally highlight the importance of orbitally forced insolation changes, and orbital precession in particular, in controlling East African hydroclimate. For instance, diatomaceous sequences within the Chemeron Formation of the Baringo Basin, located in the central Kenya Rift, suggest dramatic precessional-paced oscillations in lake levels during the late Pliocene (Deino et al., 2006; Kingston et al., 2007). Using high-precision $^{40}Ar/^{39}Ar$ ages, these studies demonstrated that the paleolake's water level varied in concert with mean summer insolation at 30°N between 2.7 and 2.55 Ma, demonstrating links between insolation and East African hydroclimate during this time period of transition and onset of Northern Hemisphere glaciation (NHG). However, variability in lake levels does not necessarily equate directly with variability in vegetation and other landscape resources.

The Baringo Basin (Fig. 1) is of particular interest because of its abundant and diverse fossil vertebrate record, which spans the last 16 Myr, providing an opportunity to explore causal links between environmental change and the evolution of hominins and their communities. The Tugen Hills succession has yielded a number of hominoid fossils (Hill and Ward, 1988; Ward et al., 1999; Rossie and Hill, 2018), including hominins (Hill, 1985; Hill et al., 1992; Sherwood et al., 2002). Outcrop $\delta^{13}C_{SC}$ records from Baringo indicate a gradual expansion of C_4 grasses over the last 10 Myr, similar to other regional

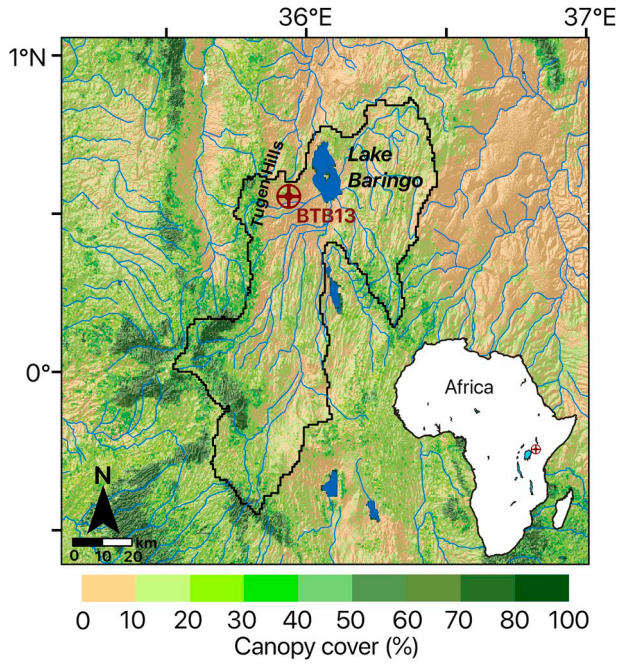

Fig. 1. Map of the modern day Baringo Basin in Northern Kenya in East Africa with the drill site of BTB13 in maroon and modern watershed outlined in black. Modern canopy cover percentage per 500 m pixel from MODIS land cover data (Hansen et al., 2003).

records (Kingston et al., 1994; Kingston, 1999). However, this gradual trend occurs with large ranges of $\delta^{13}C_{SC}$ from discrete horizons, which could suggest the presence of mixed C_3 and C_4 vegetation and/or temporally variable terrestrial ecosystems and soil carbonate formation (Kingston et al., 1994; Kingston, 1999). Higher-resolution measurements of late Pliocene vegetation trends and oscillations in the Baringo Basin could better document changes in past landscapes related to hominin evolution and broader global climate events.

The Baringo Basin provides one of the few high-resolution sedimentary successions in Africa spanning the onset of NHG at ~2.8 Ma (Zachos et al., 2001; Lisiecki and Raymo, 2005), along with critical transitions in hominin evolution (Deino et al., this issue). As part of the Hominin Sites and Paleolakes Drilling Project (HSPDP), paleolake Baringo was drilled to reconstruct regional paleoenvironments across the Plio-Pleistocene boundary. To investigate past vegetation and its response to orbital-scale rainfall oscillations during the late Pliocene, we present a novel record of $\%C_3$–$\%C_4$ vegetation based upon carbon isotopic composition of terrestrial leaf waxes derived from this core, with new hydrogen isotopic data from the same waxes (Fig. 2).

2. Regional setting and methods

The 228 m-long HSPDP-BTB13-1A drill core, hereafter BTB13, was taken from the Baringo Basin to the west of modern day Lake Baringo in central Kenya (0°33′16.56″N, 35°56′15.00″E) with a recovery of 94% (Cohen et al., 2016; Campisano et al., 2017). The lower portion of BTB13 provides lithologic evidence of fluviolacustrine and floodplain environments, whereas the upper portion contains a sequence of diatomites, mudstones, and other sediments similar to the outcrop records of deep lake cycles linked to orbital precession and eccentricity (Deino et al., 2006; Kingston et al., 2007; Cohen et al., 2016; Campisano et al., 2017). Age constraints for the core are based on $^{40}Ar/^{39}Ar$ dating of tephra deposits (Deino et al., this issue), tephrochronology (Garello et al., this issue), paleomagnetic reversals (Sier et al., this issue), and links with outcrops (Deino et al., this issue). A Bayesian stratigraphic age model incorporating these age constraints provides reference ages

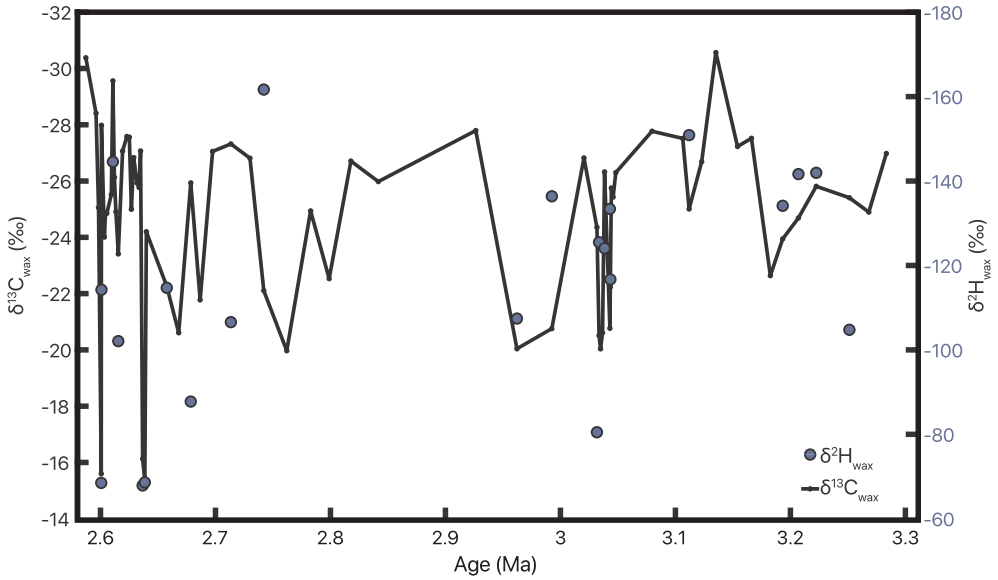

Fig. 2. Leaf wax isotope data from the BTB13 drill core from the Baringo Basin, Kenya, including $\delta^{13}C_{wax}$ (left axis, black) and $\delta^{2}H_{wax}$ (right axis, blue). (For interpretation of the references to colour in this figure legend, the reader is referred to the Web version of this article.)

and uncertainties for the entire core length (Deino et al., this issue). The core spans ~710,000 years, from 3.29 to 2.58 Ma, a period encompassing the mid-Piacenzian Warm Period (mPWP), the onset of Northern Hemisphere permanent ice and glacial cycles, the Plio-Pleistocene boundary, and origins of the *Paranthropus* and *Homo* lineages.

We analyzed the carbon isotopic composition of leaf wax biomarkers to obtain a record of the relative abundances of C_3 and C_4 vegetation in the 3.3–2.6 Ma interval (Table S1). Plants produce waxy cuticles on their surfaces to limit leaf evaporation and physical damage (Eglinton and Hamilton, 1967). These waxes may be ablated and transported by wind or water to lake sediments, where they are preserved over geological time. Plant epicuticular waxes include long-chain *n*-alkanoic acids, which were analyzed in this study, and are primarily derived from waxes of higher terrestrial plants, rather than aquatic sources (Eglinton and Hamilton, 1967; Volkman et al., 1998; Sachse et al., 2012). C_3 and C_4 plants produce distinct carbon isotopic compositions of leaf waxes during plant metabolic activities (O'Leary, 1981), providing a means to utilize isotopic analyses to infer their relative abundances through time.

We obtained 65 sediment samples from undisturbed faces of split BTB13 cores; the samples integrate up to 10 cm of core depth (averaging ~330 years). Samples were obtained from throughout the core and sampling resolution varied between 0.4 kyr and 82.5 kyr, allowing us to examine both orbital-scale variability as well as secular (longer than orbital) trends. Lipids were extracted from freeze-dried and homogenized bulk sediment using a DIONEX Accelerated Solvent Extractor 350 with dichloromethane:methanol (9:1). The lipids were separated into neutral and acid fractions over an aminopropylsilyl gel column using dichloromethane:isopropanol (2:1) and ether:acetic acid (24:1). The acids were methylated using acidified methanol and the resulting fatty acid methyl esters (FAMEs) were purified via silica gel column chromatography using hexane and dichloromethane as eluents. Relative abundances of the FAMEs were quantified using an Agilent 6890 gas chromatograph (GC) equipped with a HP1-MS column (30 m × 0.25 mm × 0.25 μm) and flame ionization detector. Carbon isotopes were measured on an Agilent 6890 GC equipped with HP1-MS column (30 m × 0.25 mm × 0.10 μm) coupled to a Thermo Delta V Plus isotope ratio mass spectrometer (IRMS) with a reactor held at 1100 °C at Brown University. The IRMS was run with CO_2 as the internal standard, and a FAMEs internal standard (−17.61‰) was measured every 7th injection and yielded a standard deviation (1σ) of 0.17‰. Carbon isotope ratios were measured in duplicate on each sample with a mean inter-sample difference of 0.20‰. Hydrogen isotopic ($\delta^{2}H_{wax}$) measurements (22) were also performed according to measurement procedures from Lupien et al. (2018). The FAMEs standard (−163.85‰) had a 1σ of 1.38‰, and 10 samples were measured in triplicate with a 1σ of 1.19‰, and 12 samples were measured as single injections due to low sample concentration. All carbon and hydrogen measurements were corrected for the isotopic composition of the added methyl group, where $\delta^{13}C_{MeOH} = -36.52‰$ and $\delta^{2}H_{MeOH} = -123.7‰$. We report $\delta^{13}C_{wax}$ relative to Pee Dee Belemnite (PDB) in per mil (‰) notation and $\delta^{2}H_{wax}$ relative to Vienna Standard Mean Ocean Water.

To infer the relative abundance of C_3 and C_4 vegetation, we use a two end-member mixing model that assigns a $\delta^{13}C$ to *n*-C_{30} acids of −32.9‰ for the C_3 endmember and a $\delta^{13}C$ of *n*-C_{30} acid of −19.0‰ for the C_4 end member (Equation S(1)). These *n*-C_{30} values are based on nearby Nachukui outcrop measurements from the Turkana Basin and obtain the same (within error) average as *n*-C_{28} from the same samples, and thus do not require a isotope homologue correction (Uno et al., 2016b). It is unlikely that CAM plants, which have $\delta^{13}C_{wax}$ values intermediate between C_3 and C_4 plants, were present in high concentrations, and therefore we do not include them in the mixing model (Kingston, 1999).

We interpret the $\delta^{2}H_{wax}$ to reflect changes in precipitation amount by way of the 'amount effect,' through which times of stronger tropical rainfall cause ^{2}H-depleted precipitation (Dansgaard, 1964; Rozanski et al., 1993). ^{2}H-enriched water is preferentially lost from atmospheric water vapor during times of stronger rainfall as a result of a series of Rayleigh fractionation processes (Dansgaard, 1964). Terrestrial plants utilize soil water for photosynthesis and their leaf waxes record the $\delta^{2}H_{precip}$ with a linear offset (Sachse et al., 2004; Garcin et al., 2012).

In addition to carbon isotope data from leaf waxes, bulk organic matter (OM) carbon isotope analyses ($\delta^{13}C_{OM}$) were performed at the University of Arizona to provide more continuous OM records through intervals in which leaf wax data were unavailable or occur at lower temporal resolution. Dried sediments were powdered and acidified in beakers with 1 N HCl acid. Reaction was deemed complete when pH after the reaction was less than 7. Sediments were then filtered with 0.4 μm filters and rinsed with distilled water. $\delta^{13}C$, as well as $\delta^{15}N$ and carbon and nitrogen content (Table S2), were measured on a continuous-flow gas-ratio mass spectrometer (Finnigan Delta PlusXL). Samples were combusted using an elemental analyzer (Costech) coupled to the mass spectrometer. Standardization is based on NBS-22 (−30.03‰) and USGS-24 (−16.05‰) for $\delta^{13}C_{OM}$. $\delta^{13}C_{OM}$ is also

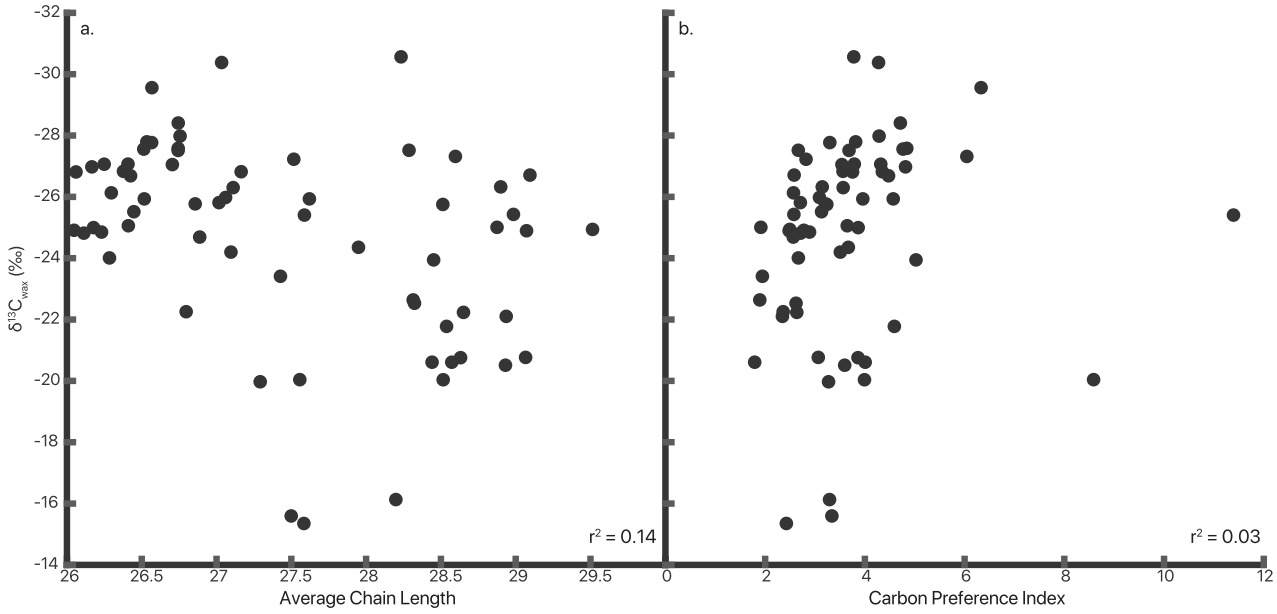

Fig. 3. Cross-plot correlations of $\delta^{13}C_{wax}$ and ACL (a) and CPI (b).

presented in per mil notation relative to PDB. The bulk organic matter incorporates carbon from both the landscape and the lake itself, and its isotopic composition incorporates a variety of signals of both aquatic and terrestrial environmental processes (Meyers and Ishiwatari, 1993; Meyers and Lallier-Vergès, 1999; Meyers, 2003; Talbot et al., 2006; Eglinton and Eglinton, 2008; Russell et al., 2009; Webb et al., 2016). Correlation between $\delta^{13}C_{OM}$ and $\delta^{13}C_{wax}$ was performed by using the nearest $\delta^{13}C_{OM}$ measurement within 500 years of a $\delta^{13}C_{wax}$ measurement.

Time series and statistical tools were used to analyze trends and patterns within the isotope record. Data was resampled to an even time-step and used the findchangepts tool from the Signal Processing Toolbox in MATLAB (MathWorks, 2018a) to determine statistically robust change points in the record, i.e. the timing of changes in the mean of the $\delta^{13}C_{wax}$ and $\delta^{13}C_{OM}$ records. This function creates a step-wise model with a cost penalty for each additional change point in order to most effectively reduce the residual mean squared error to find the optimal timing and number of change points. To avoid overfitting the data, we employed minimum bounds on the residual error and the number of points between each step.

3. Results

$\delta^{13}C$ values of different leaf wax homologues were strongly positively correlated (C_{28} and C_{26} $r = +0.87$, $p < 0.01$, $n = 61$ with two C_{26} outliers removed; C_{28} and C_{30} $r = +0.90$, $p < 0.01$, $n = 62$) demonstrating that these waxes are derived from a common source (i.e. higher plants) in the BTB13 sediment samples. We use the $\delta^{13}C_{wax}$ and $\delta^{2}H_{wax}$ of C_{28} *n*-alkanoic acid for all analyses because of its high abundance, which results in a lower analytical error and higher number of measurements. $\delta^{2}H_{wax}$ averages −115.2‰ and varies from −67.9‰ to −161.7‰, a range of nearly 100‰.

$\delta^{13}C_{wax}$ averages −24.7‰ in the BTB13 record, and the values range from −15.4 to −30.6‰ (Fig. 2), similar to the range of the $\delta^{13}C_{wax}$ of *n*-C_{28} acids in C_3 and C_4 endmembers (Chikaraishi and Naraoka, 2007). The Average Chain Length (ACL) of the long chain *n*-alkanoic acids (C_{24}–C_{32}) is 27.4, similar to modern East African lake sediment samples (Fig. 3a; Vogts et al., 2009; Garcin et al., 2012; Uno et al., 2016a). The Carbon Preference Index (CPI; Bray and Evans, 1961) values averaged 3.6 (C_{16}–C_{32}), well above highly degraded hydrocarbons (oil) values of 1 (Fig. 3b). Throughout our core, CPI and $\delta^{13}C_{wax}$ values are uncorrelated ($r = +0.17$, $p > 0.05$, $n = 65$), suggesting degradation has little effect on the isotopic composition of these waxes. Long chain ACL (C_{24}–C_{32}) and $\delta^{13}C_{wax}$ are significantly, yet weakly, correlated ($r = +0.38$, $p < 0.01$, $n = 65$), in keeping with previous work suggesting that grasses produce longer chain lengths (e.g. Cranwell, 1973).

Our $\delta^{13}C_{wax}$ record implies vegetation ranged from 0% to ~83% C_3. We observe some samples with $\delta^{13}C_{wax}$ values more enriched than the C_4 endmember value that yield negative $\%C_3$ values, and manually adjusted these to as 0% C_3. Many of these have $\delta^{13}C_{wax}$ values near the C_4 endmember, but three samples have $\delta^{13}C_{wax}$ near −16‰, outside of this range. It is possible that these three samples may have contained waxes from aquatic plants, though their ACL and CPI values do not support this. These values are removed in the resampling procedure and do not affect our statistical analyses.

$\delta^{13}C_{OM}$ averages −23.12‰ in the BTB13 record, and the values range from −7.80‰ to −28.75‰, values that are more enriched than our long-chain $\delta^{13}C_{wax}$ values. The $\delta^{13}C$ of bulk organic matter is often more enriched than $\delta^{13}C_{wax}$. This can result from more enriched aquatic signature incorporated into the sedimentary organic matter (Meyers, 2003), although it should also be noted that the $\delta^{13}C$ bulk terrestrial plant biomass is enriched relative to the $\delta^{13}C$ of co-occurring waxes (Collister et al., 1994).

The correlation between $\delta^{2}H_{wax}$ and $\delta^{13}C_{wax}$ through the Chemeron Formation 2.7–2.55 Ma is highly significant ($r = +0.88$, $p < 0.01$, $n = 8$; Fig. 2). The correlation between $\delta^{13}C_{wax}$ and $\delta^{13}C_{OM}$ throughout the core is less strongly significant ($r = +0.50$, $p < 0.05$, $n = 22$), but the two show generally similar patterns and trends in the core (Fig. 4). We use the $\delta^{13}C_{OM}$ data (228 samples) to compare statistical analyses of the highly resolved record and the lower resolution $\delta^{13}C_{wax}$ record (Fig. 4).

4. Discussion

4.1. C_4 expansion in the Baringo Basin

Multiple studies of terrestrial vegetation have shown that C_4 grasslands gradually expanded since the Miocene in East Africa (Cerling and Hay, 1986; Cerling, 1992; Kingston et al., 1994; Kingston, 1999; Bobe et al., 2002; Bobe and Behrensmeyer, 2004; Feakins, 2013; Liddy et al., 2016; Uno et al., 2016a). Paleoenvironmental records from leaf waxes, soil carbonates, and pollen also indicate that Pliocene landscapes in East Africa were more wooded and contained less C_4 grasses than today

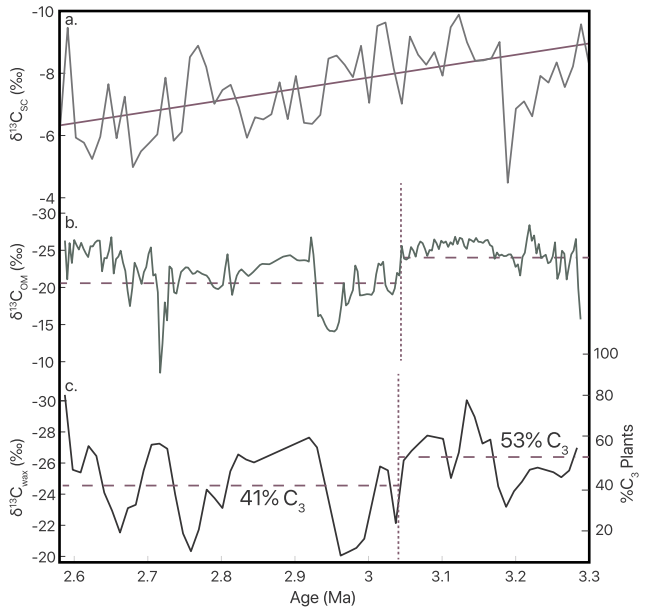

Fig. 4. Linearly resampled carbon isotope records from eastern African soil carbonate (a; Levin, 2013 and references therein), BTB13 bulk organic matter (b; this study), and BTB13 leaf wax (c; this study). Resampling was necessary for change point analysis, which resulted in change with stronger significance than a simple linear regression in the $\delta^{13}C_{OM}$ and $\delta^{13}C_{wax}$ records, whereas the East African $\delta^{13}C_{SC}$ compilation record demonstrates a highly significant trend towards C_4 plants. Change point analyses of the $\delta^{13}C_{OM}$ and $\delta^{13}C_{wax}$ records produce single shifts (purple dashed line) at the same time ~3.04 Ma, signifying a robust change in Baringo Basin vegetation type at this time. (For interpretation of the references to colour in this figure legend, the reader is referred to the Web version of this article.)

(White, 1983; Cerling et al., 2011), consistent with interpretations from offshore records of long-term regional drying (deMenocal, 1995). The expansion of C_4 grasses in Africa is generally thought to be gradual (Cerling et al., 1997; Feakins et al., 2005; Feakins, 2013; Levin, 2015; Uno et al., 2016a), although many of the existing records have a low temporal resolution that cannot capture abrupt changes or the nature of the transition. High-resolution marine dust records suggest step-wise shifts towards aridity at specific intervals, including a transition at ~2.8 Ma, which suggest a potential link between landscape changes and the onset of Northern Hemisphere Glaciation (NHG; deMenocal, 1995). Given the significance of this transition in global climate as well as implications for hominin and bovid evolution, it has been proposed that a step change towards more arid-adapted vegetation in Africa may have occurred as a coordinated pulse at this time (Vrba, 1985, 1995; deMenocal, 1995, 2004; Maslin and Trauth, 2009). However, more direct measurements of Pliocene vegetation structure (e.g. Rose et al., 2016) vary in their resolution and source area, complicating our interpretations of C_4 expansion and its relationship to global climate.

East African $\delta^{13}C_{SC}$ records demonstrate a significant ($p < 0.01$) trend toward more C_4 vegetation between 3.3 and 2.6 Ma (Fig. 4a; Levin, 2013 and references therein). The long-term, gradual C_4 expansion documented by these data since ~4 Ma demonstrates little connection to the relatively rapid onset of NHG at 2.8 Ma (Levin, 2013 and references therein). However, when basins are examined individually, most have at least one step-wise shift towards C_4 grasses in the Plio-Pleistocene, in addition to or even rather than a gradual secular trend. These basin-scale $\delta^{13}C_{SC}$ shifts occur at different times (e.g. the Afar shifts at ~3 Ma, Omo-Turkana at ~1.9 Ma; Levin, 2013 and references therein) suggesting that basin-specific attributes dictate the timing and nature of vegetation responses. If so, these records could suggest C_4 grasses expanded when local climates crossed critical thresholds within individual basins, as global climate cooled, became drier, and decreased in CO_2 (Polissar et al., 2019). Marine records of terrestrial vegetation, which integrate much larger continental-scale source areas than paleosol carbonates, vary during this interval. These data indicate either a gradual trend towards a more open environment since ~4 Ma, well before the onset of NHG (Feakins et al., 2013), or little change in vegetation between the Pliocene and Pleistocene (Rose et al., 2016).

Carbon isotopic records from paleosol carbonates and organic matter in the Baringo Basin suggest that the rift valley floor in this region was covered by ~70% C_3 forests in the late Pliocene, and then gradually shifted to more open grasslands that are present in the area today (Fig. 5c; Kingston et al., 1994; Kingston, 1999). Whereas the $\delta^{13}C_{SC}$ from the Baringo Basin is currently too sparse to characterize or identify the exact timing of changes over the study interval, the Pliocene was interpreted as a consistently heterogenous landscape prior to hominin turnover events and the onset of NHG occurring at the Plio-Pleistocene boundary (Kingston et al., 1994; Kingston, 1999). Our $\delta^{13}C_{wax}$ record documents significant changes in the relative abundance of C_3 and C_4 vegetation during the late Pliocene and early Pleistocene in the Baringo Basin. Although there is no statistically significant linear trend ($p > 0.7$), change point analyses indicate a shift in $\delta^{13}C_{wax}$ at ~3.04 Ma (Fig. 4c). C_3 abundances prior to 3.04 Ma averaged 53% but averaged 41% afterwards. The absolute $\%C_3$ values are sensitive to the endmembers chosen for $\delta^{13}C_{wax}$, and the low temporal resolution of our sampling could limit the ability to determine the precise timing of the

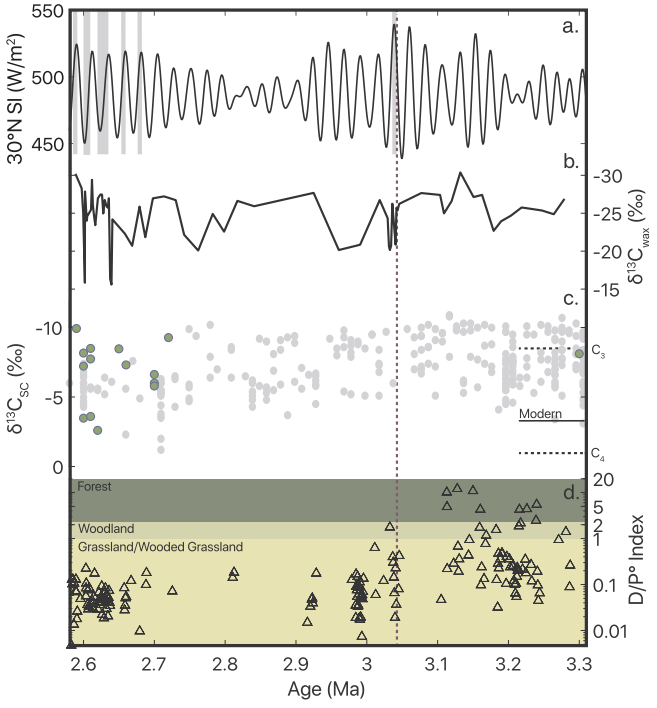

Fig. 5. BTB13 $\delta^{13}C_{wax}$ (b) compared to mean summer 30°N insolation (a; Laskar et al., 2004) containing the characteristic diatomaceous sequence from the Chemeron Formation (light grey bands) in the Baringo Basin (Deino et al., 2006; Kingston et al., 2007). Wax isotopes are further contextualized with $\delta^{13}C_{SC}$ measurements (c) from the Baringo Basin (green circles; Kingston et al., 1994; Kingston, 1999) and the East African compilation (grey circles; Levin, 2013 and references therein). C_3 and C_4 endmembers (dashed lines) and modern value from the Baringo Basin demonstrate that the late Pliocene was on average more C_3-dominated than today (c). Vegetation reconstructions from the ratio of tree:grass phytoliths (triangles; Yost et al., this issue) produce an index of tree cover D/P° (d). The D/P° index (Bremond et al., 2008) is a proxy for tree canopy cover in Africa and has been applied to determine vegetation structure, with vegetation formation classifications after White (1983). The changepoint-derived shift in vegetation at ~3.04 Ma is denoted in purple dashed line. (For interpretation of the references to colour in this figure legend, the reader is referred to the Web version of this article.)

shift, but the analysis indicates that a significant mean shift occurred. $\delta^{13}C_{OM}$ exhibits a moderately significant trend ($p < 0.05$) towards less negative values, and it exhibits a change point toward less negative values at 3.04 Ma (Fig. 4b), the same time as the $\delta^{13}C_{wax}$ shift. Although the $\delta^{13}C_{OM}$ responds to multiple environmental processes, including carbon cycling in aquatic and terrestrial ecosystems (Meyers and Ishiwatari, 1993), the similarity of $\delta^{13}C_{wax}$ and $\delta^{13}C_{OM}$ changepoints suggests major changes in aquatic and terrestrial paleoenvironments in the Baringo Basin at ~3.04 Ma. Moreover, phytolith analyses show a change in vegetation structure at about this time (Fig. 5d; Yost et al., this issue). Specifically, the ratio of tree:grass phytoliths (D/P° index; Bremond et al., 2008; Yost et al., 2018) shows evidence of woody vegetation in the Baringo Basin before 3.1 Ma, and more open grasslands and a lack of forested vegetation after 3.04 Ma (Yost et al., this issue. Limited pollen data from BTB13 also support this finding (Yost et al., this issue).

Although the timing of vegetation change in the Baringo Basin at ~3.04 Ma is close to the timing of the onset of NHG at ~2.8 Ma, the shift appears to predate it by ~200 kyr. This offset is not an artifact of the BTB13 age model, which is tightly controlled in this interval by $^{40}Ar/^{39}Ar$ ages from core and outcrop (Deino et al., this issue), and paleomagnetic reversal stratigraphy (Sier et al., this issue). Median model uncertainties are ±0.03 Ma at the 95% confidence interval (Deino et al., this issue). The age of the transition is well-constrained with a Bayesian age model that provides a 95% confidence interval of less than 100 kyr (Deino et al., this issue). Thus, our record suggests that vegetation change in this region predated the onset of NHG. This could indicate that climate in this region shifted prior to the onset of NHG, perhaps associated with the termination of the mPWP, but it is also possible that the change in vegetation is related to basin-specific geomorphic processes and/or threshold responses of vegetation to long-term changes in East African climate.

Sedimentological evidence from BTB13 suggests that there was a major change in basin geometry beginning about the same time as the paleoecological shift in $\delta^{13}C_{wax}$. For instance, the first diatomite in BTB13 occurs at 3.04 Ma (Westover et al., this issue). This sedimentological marker indicates a change in the types of lake deposits, shown in part by magnetic susceptibility (Scott et al., this issue) and a reduction in sedimentation rate (~3.04–2.7 Ma; Deino et al., this issue), and culminates in regular diatomite sequences by ~2.7 Ma which may represent a stable basin with greater accommodation space for deep lakes to occur during strong monsoons (Fig. 5a; Deino et al., 2006; Kingston et al., 2007). The change in zeolite facies at ~3 Ma also indicates a change in the water chemistry of the paleolake system (Minkara et al., this issue). Increased basin subsidence could promote more extensive low-lying, flood-prone land in the Baringo Basin, and thus more C_4 grasses or sedges contributing to the $\delta^{13}C_{wax}$ signal. Similar shifts have been observed in Lake Tanganyika and Lake Malawi (Ivory et al., 2016; Ivory and Russell, 2016), where lake lowstands and basin reconfigurations promote sedge expansion on low-lying areas and contribute ^{13}C-enriched waxes to the sedimentary record.

Alternatively, it is possible that the shift in vegetation was caused by a rapid shift in climate at ~3.04 Ma. If so, climate changes in this region may predate the onset of NHG, and instead result from other climate forcings, such as the termination of the mPWP (De Schepper et al., 2014). The clearest evidence for climate as the main control on $\delta^{13}C_{wax}$ derives from data in the upper ~40 m of the BTB13 core, where $\delta^{13}C_{wax}$ exhibits clear relationships with orbital-scale lake level variations marked by diatom-rich layers (Fig. 5a; Westover et al., this issue; Scott et al., this issue; Deino et al., this issue) and also exhibits a strong, positive correlation with $\delta^{2}H_{wax}$ ($r = +0.88$, $p < 0.01$, $n = 8$). The $\delta^{2}H_{wax}$ record thus indicates that increased rainfall is associated with expansion of C_3-dominated ecosystems (Fig. 2). This coupling suggests that the vegetation changes in the Baringo Basin at orbital time-scales are controlled, at least in part, by changes in precipitation. Although this suggests climate could also control the shift at ~3.04 Ma, it is not clear whether the processes controlling vegetation change at orbital time-scales are the same as those operating on long time-scales. Because of low wax concentrations near 3.04 Ma, we were unable to generate $\delta^{2}H_{wax}$ data over this transition and across the crucial interval of the onset of NHG. More $\delta^{2}H_{precip}$ data is needed to test the climatic impact on the Baringo Basin.

It is also possible that the $\delta^{13}C_{wax}$ signal records a relatively rapid, non-linear vegetation change in response to gradual climate forcings. The gradual CO_2 decline (Kürschner et al., 1996; Raymo et al., 1996; Tripati et al., 2009; Pagani et al., 2010; Seki et al., 2010; Bartoli et al., 2011; Badger et al., 2013), aridification (deMenocal, 1995), or cooling (Herbert et al., 2010) during the Plio-Pleistocene could all drive environmental changes in East Africa. pCO_2 and temperature have a large effect on plant metabolic pathways, and could result in step-changes in the relative abundance of C_3 vs. C_4 plants (Hatch, 1987). Another possibility is an increase in rainfall seasonality (longer dry season) at this time. C_4 grasses are better suited for a strongly seasonal rainfall than C_3 plants (Ivory et al., 2012), such that increased seasonality could trigger a response in vegetation that would not be predicted from changes in mean annual precipitation amount alone (Hély et al., 2006). Indeed, the appearance of diatomites in the BTB13 succession at this time (~3.04 Ma) would, to first order, suggest a wetter climate that would likely favor C_3 vegetation, not C_4 grasses.

The shift toward C_4 vegetation recorded by $\delta^{13}C_{wax}$ at ~3.04 Ma likely reflects a variety of environmental and climatic signals experienced by the Baringo Basin, including tectonically driven changes in basin geomorphology and long-term changes in East African and global climate, which may have been acting in concert. The onset of NHG post-dates this environmental transition, although global cooling prior to and across the Plio-Pleistocene boundary likely played a role. Future high-resolution reconstructions of precipitation may shed light on these processes.

4.2. Highly variable vegetation at orbital timescales

An emerging body of hydroclimate records have begun to document the amplitude and periodicity of rainfall variations in East Africa during the Plio-Pleistocene. Long, continuous records of Mediterranean sapropel formation (Rossignol-Strick, 1983, 1985; Grant et al., 2017) and East African lake levels (Trauth et al., 2005; Kingston et al., 2007; Maslin and Trauth, 2009; Nutz et al., 2017) show that hydroclimate variability correlates strongly with orbital precession during the Pliocene and Pleistocene, just as it did during the last deglaciation and the late Pleistocene/Holocene African Humid Period (deMenocal et al., 2000; Otto-Bliesner et al., 2014; Shanahan et al., 2015). Geochemical records of monsoon strength from leaf waxes (Rose et al., 2016; Lupien et al., 2018) and strontium isotopes (Joordens et al., 2011) also indicate that the 21-kyr precession cycle dominates these hydroclimatic records.

In contrast, records of vegetation change typically lack the resolution to evaluate orbital-scale vegetation changes. The $\delta^{13}C_{SC}$ records typically have very large ranges within single stratigraphic horizons, limiting their utility at orbital timescales. Records that are able to resolve orbital cycles demonstrate precession-band variability in vegetation type (e.g. Rose et al., 2016). However, existing records disagree on the amplitude of variability: marine cores suggest fluctuations of ~20% between C_3 and C_4 vegetation on orbital timescales (Feakins and Eglinton, 2007; Rose et al., 2016), whereas terrestrial records demonstrate ~70% fluctuation between C_3 and C_4 endmembers (Magill et al., 2013; Lupien et al., 2018). Most of these records are from the early Pleistocene, with the late Pliocene prior to the onset of NHG left understudied.

Previous studies of Baringo Basin vegetation have been limited to low-resolution paleosol organic matter and carbonate $\delta^{13}C$ (Fig. 5c; Kingston et al., 1994; Kingston, 1999). Similar to $\delta^{13}C_{SC}$ from other basins, the Baringo Basin demonstrates a large range of lateral variability. This variability has been interpreted to reflect a heterogenous landscape with mixed C_3/C_4 vegetation (Kingston et al., 1994; Kingston, 1999). However, it is also possible that these carbonate

nodules formed at similar depths in soil horizons but at different times, such that the range of values reflects high-amplitude changes in vegetation at short time-scales.

Indeed, we observe very high-amplitude $\delta^{13}C_{wax}$ fluctuations, indicating variations from 80% to 0% C_3 in the BTB13 core (Fig. 4c). Prior to the mean shift at ~3.04 Ma, $\delta^{13}C_{wax}$ fluctuated between ~80% and ~20% C_3 plants, and after ~3.04 Ma, the vegetation ranges from ~60% to 0% C_3. Indeed, near the shift in mean at ~3.04 Ma, there is a very large oscillation from ~80 to 0% C_3. As discussed above, the covariation of $\delta^{13}C_{wax}$ with $\delta^{2}H_{wax}$ strongly implicates climate as the trigger of these vegetation shifts. Moreover, higher-resolution analyses of $\delta^{13}C_{wax}$ values through the diatomaceous facies alternations in the upper Chemeron Formation (Fig. 5a; top 40 m of BTB13), which have been linked with variations in lake level and changing monsoon strength at the precession band (Deino et al., 2006; Kingston et al., 2007), show that C_3 plants were more abundant during lake highstands. Additionally, the phytolith record from BTB13 indicates that C_4 grass community composition shifted between mesic- and xeric-dominated taxa at precessional periodicity (Yost et al., this issue). This demonstrates that vegetation change was closely linked with hydroclimate and that, in the latest Pliocene, climate and environment fluctuated at a ~21-kyr periodicity. Although the sampling resolution of our leaf wax records prior to the D1 diatomite interval is relatively low, we postulate that precession-band variation likely occurred throughout this interval, dramatically oscillating between C_3- and C_4-dominated ecosystems.

By coupling carbon and hydrogen isotopic analyses from waxes, we show that vegetation in the Plio-Pleistocene Baringo Basin was highly sensitive to hydroclimate change. Following the onset of NHG at ~2.8 Ma, glacial-interglacial cycles began to vary at the obliquity band (Lisiecki and Raymo, 2005). Although our $\delta^{13}C_{wax}$ record lacks the length and resolution to exclude obliquity-based variations, we show large vegetation changes accompanied precession-band changes in East African hydroclimate. Moreover, the amplitude of vegetation changes at orbital timescales is much larger than the secular change we see at ~3.04 Ma, whether the shift was caused by basin geomorphic changes or even nonlinear responses to gradual climate change.

4.3. Hominin evolution in the late Pliocene

Early hominins relied on vegetation for shelter, food, hunting, technological resources, and migration passages (Vrba, 1985). Physiological changes, such as expansion of the cerebral cortex (Tobias, 1995; Shultz et al., 2012) and technological advances such as the first butchery sites (Asfaw et al., 1999), occurred in the late Pliocene. A major turnover in hominin lineage from *Australopithecus* to *Homo* and *Paranthropus* appears to have occurred during the late Pliocene (Potts, 2013 and references therein), although first and last appearance dates (FADs and LADs) of hominin species are still poorly constrained. Fossil evidence from a *Homo* mandible puts the FAD of the genus at ~2.8 Ma (Villmoare et al., 2015), but stone tools that are typically associated with *Homo* were recently discovered and dated to ~3.3 Ma (Harmand et al., 2015). Although this latter find is not direct fossil evidence of hominin material, a number of these transitions in hominin evolution coincide with major increases in animal diversification (Bobe et al., 2002), suggesting evolutionary responses of multiple mammalian lineages to major environmental changes (deMenocal, 1995; Potts, 1996, 1998).

The long, continuous record of vegetation described here enables a more comprehensive understanding of the environmental context in which our hominin ancestors lived. Hypotheses reliant on changes in mean climate state posit that long-term (*savannah hypothesis*; Dart, 1925; Domínguez-Rodrigo et al., 2013) or short-term (*turnover pulse hypothesis*; Vrba, 1985, 1993) secular trends/shifts towards open vegetation drive hominin evolution. Others point to the amplitude of paleoclimate variability, such as orbitally driven transitions between humid and arid climates, as the driver of hominin turnover and dispersal (Potts, 1996). The *variability selection hypothesis* posits that high-amplitude environmental variability selects for species that are better-equipped to live in or travel to a variety of environments (Potts, 1996, 1998; Maslin and Trauth, 2009; Potts and Faith, 2015). All hypotheses are in part supported by existing data from paleoenvironmental records.

In the BTB13 core leaf wax record, the ~10% increase in C_4 vegetation at ~3.04 Ma could indicate an environmental change of sufficient magnitude to generate selective forces leading to some of the key hominin evolutionary events. However, our record is noteworthy for the very large environmental changes and temporally heterogeneous landscapes that characterized the Baringo Basin during both the late Pliocene and early Pleistocene. Moreover, although our $\delta^{13}C_{wax}$ record senses vegetation differently than $\delta^{13}C_{sc}$ records do, it suggests that vegetation transitions were not synchronous across East Africa. Whereas our $\delta^{13}C_{wax}$ record indicates a pulse of C_4 expansion at about 3.04 Ma, $\delta^{13}C_{SC}$ records from Awash and the Turkana basin suggest C_4 expansion beginning at about 2.7 and 2.0 Ma, respectively. Such regional heterogeneity seems inconsistent with the *turnover pulse hypothesis*. The lack of high resolution throughout the BTB13 record prevents us from directly testing the *variability selection hypothesis*, yet it is clear from the $\delta^{13}C_{wax}$ record that orbital-scale (or shorter) variability was much larger than long-term secular changes. Such extreme environmental oscillations would likely play a large role in hominin evolution.

5. Conclusions

New $\delta^{13}C_{wax}$ and $\delta^{2}H_{wax}$ records from the Baringo Basin, Kenya provide new terrestrial vegetation and hydroclimate information from the late Pliocene (3.3–2.6 Ma). The reconstructions characterize East African environmental trends and oscillations and provide a means of testing hominin evolutionary hypotheses. The $\delta^{13}C_{wax}$ record indicates that mixed C_3 and C_4 vegetation existed in the Baringo Basin through much of this time interval. A ~10% increase in C_4 vegetation was documented at ~3.04 Ma, which predates the onset of Northern Hemisphere Glaciation. This transition could have been the result of geomorphic evolution of the Baringo Basin, or by a nonlinear response of vegetation to changes in pCO_2, temperature, precipitation, or precipitation seasonality at this time. $\delta^{13}C_{wax}$, $\delta^{2}H_{wax}$, and diatomaceous sequences show strong correlations in the upper part of the BTB13 core and indicate that precipitation cycles forced by orbital precession caused large changes in the relative abundance of C_3 versus C_4 vegetation. The relative amplitude of orbital-scale variability is much larger than the secular shift in vegetation occurring at ~3.04 Ma, suggesting that orbitally driven insolation changes had a much larger impact on East African climate and environments than gradual changes in global climate.

The shift in mean vegetation at ~3.04 Ma, and the persistently high environmental variability throughout our record, suggest that high-frequency, high-amplitude changes in vegetation could have been the environmental stressor that drove hominin evolutionary transitions. Whereas conclusive support for a particular evolutionary hypothesis is lacking, there is more room for reconstructions of continuous and highly resolved climate records to address questions about global and local influences on environment and hominins. The BTB13 archive of hydroclimate and vegetation provides crucial understanding of Plio-Pleistocene climate and evolution of East African ecosystems.

Declaration of competing interest

The authors declare that the research was conducted in the absence of any commercial or financial relationships that could be construed as a potential conflict of interest.

Acknowledgements

We wish to thank Tristan Reinecke and Dheivanai Moorthy for sample preparation, Marcelo Alexandre, Rafael Tarozo, and Ewerton Santos for laboratory assistance, and the members of the Hominin Sites

and Paleolakes Drilling Project (HSPDP) for useful discussions. Support for HSPDP has been provided by the National Science Foundation (NSF) grants EAR 1322017, EAR 1338553, BCS 1241790, and the International Continental Drilling Program (ICDP). Research and drilling permits were provided by the Kenyan National Council for Science and Technology, the Kenyan Ministry of Mines, and the National Environmental Management Authority of Kenya, and facilitated by the National Museums of Kenya. We thank DOSECC Exploration Services for drilling supervision and Drilling and Prospecting International (DPI) for drilling services. Initial core processing and sampling were conducted at the US National Lacustrine Core Facility (LacCore) at the University of Minnesota. Data are freely available at the World Data Center-A for Paleoclimatology. We thank anonymous reviewers for helpful comments on an earlier version of this manuscript. This is publication 22 of the Hominin Sites and Paleolakes Drilling Project.

Appendix A. Supplementary data

Supplementary data to this article can be found online at https://doi.org/10.1016/j.palaeo.2019.109426.

References

Asfaw, B., White, T., Lovejoy, O., Latimer, B., Simpson, S., Suwa, G., 1999. Australopithecus garhi: a new species of early hominid from Ethiopia. Science 284, 629–635.

Badger, M.P., Schmidt, D.N., Mackensen, A., Pancost, R.D., 2013. High-resolution alkenone palaeobarometry indicates relatively stable pCO2 during the Pliocene (3.3–2.8 Ma). In: Philosophical Transactions of the Royal Society of London A: Mathematical, Physical and Engineering Sciences, vol. 371. pp. 20130094.

Bartoli, G., Hönisch, B., Zeebe, R.E., 2011. Atmospheric CO2 decline during the Pliocene intensification of northern Hemisphere glaciations. Paleoceanography 26.

Bobe, R., Behrensmeyer, A.K., 2004. The expansion of grassland ecosystems in Africa in relation to mammalian evolution and the origin of the genus Homo. Palaeogeogr. Palaeoclimatol. Palaeoecol. 207, 399–420.

Bobe, R., Behrensmeyer, A.K., Chapman, R.E., 2002. Faunal change, environmental variability and late Pliocene hominin evolution. J. Hum. Evol. 42, 475–497.

Bonnefille, R., 2010. Cenozoic vegetation, climate changes and hominid evolution in tropical Africa. Glob. Planet. Chang. 72, 390–411.

Bray, E., Evans, E., 1961. Distribution of n-paraffins as a clue to recognition of source beds. Geochem. Cosmochim. Acta 22, 2–15.

Breecker, D., Sharp, Z., McFadden, L.D., 2009. Seasonal bias in the formation and stable isotopic composition of pedogenic carbonate in modern soils from central New Mexico, USA. Geol. Soc. Am. Bull. 121, 630–640.

Bremond, L., Alexandre, A., Wooller, M.J., Hély, C., Williamson, D., Schäfer, P.A., Majule, A., Guiot, J., 2008. Phytolith indices as proxies of grass subfamilies on East African tropical mountains. Glob. Planet. Chang. 61, 209–224.

Campisano, C.J., Cohen, A.S., Arrowsmith, J.R., Asrat, A., Behrensmeyer, A.K., Brown, E.T., Deino, A.L., Deocampo, D.M., Feibel, C.S., Kingston, J.D., Lamb, H., Lowenstein, T.K., Noren, A., Olago, D.O., Owen, R.B., Pelletier, J.D., Potts, R., 2017. The hominin sites and paleolakes drilling project: high-resolution paleoclimate records from the east African rift system and their implications for understanding the environmental context of hominin evolution. PaleoAnthropology 1, 43.

Campisano, C.J., Feibel, C.S., 2007. Connecting local environmental sequences to global climate patterns: evidence from the hominin-bearing Hadar Formation, Ethiopia. J. Hum. Evol. 53, 515–527.

Cerling, T.E., 1992. Development of grasslands and savannas in East Africa during the neogene. Palaeogeogr. Palaeoclimatol. Palaeoecol. 97, 241–247.

Cerling, T.E., Harris, J.M., MacFadden, B.J., Leakey, M.G., Quade, J., Eisenmann, V., Ehleringer, J.R., 1997. Global vegetation change through the Miocene/Pliocene boundary. Nature 389, 153.

Cerling, T.E., Hay, R.L., 1986. An isotopic study of paleosol carbonates from Olduvai Gorge. Quat. Res. 25, 63–78.

Cerling, T.E., Wynn, J.G., Andanje, S.A., Bird, M.I., Korir, D.K., Levin, N.E., Mace, W., Macharia, A.N., Quade, J., Remien, C.H., 2011. Woody cover and hominin environments in the past 6 million years. Nature 476, 51.

Chikaraishi, Y., Naraoka, H., 2007. $\delta^{13}C$ and δD relationships among three n-alkyl compound classes (n-alkanoic acid, n-alkane and n-alkanol) of terrestrial higher plants. Org. Geochem. 38, 198–215.

Cohen, A., Campisano, C., Arrowsmith, R., Asrat, A., Behrensmeyer, A., Deino, A., Feibel, C., Hill, A., Johnson, R., Kingston, J., Lamb, H., Lowenstein, T., Noren, A., Olago, D., Owen, R.B., Potts, R., Reed, K., Renaut, R., Schäbitz, F., Tiercelin, J.-J., Trauth, M., Wynn, J., Ivory, S., Brady, K., O'Grady, R., Rodysill, J., Githiri, J., Russell, J., Foerster, V., Dommain, R., Rucina, S., Deocampo, D., Russell, J., Billingsley, A., Beck, C., Dorenbeck, G., Dullo, L., Feary, D., Garello, D., Gromig, R., Johnson, T., Junginger, A., Karanja, M., Kimburi, E., Mbuthia, A., McCartney, T., McNulty, E., Muiruri, V., Nambiro, E., Negash, E., Njagi, D., Wilson, J., Rabideaux, N., Raub, T., Sier, M., Smith, P., Urban, J., Warren, M., Yadeta, M., Yost, C., Zinaye, B., 2016. The Hominin Sites and Paleolakes Drilling Project: inferring the environmental context of human evolution from eastern African rift lake deposits. Sci. Drill. 21, 1.

Collister, J.W., Rieley, G., Stern, B., Eglinton, G., Fry, B., 1994. Compound-specific δ13C analyses of leaf lipids from plants with differing carbon dioxide metabolisms. Org. Geochem. 21, 619–627.

Cranwell, P.A., 1973. Chain-length distribution of n-alkanes from lake sediments in relation to post-glacial environmental change. Freshw. Biol. 3, 259–265.

Dansgaard, W., 1964. Stable isotopes in precipitation. Tellus 16, 436–468.

Dart, R.A., 1925. Australopithecus africanus: the man-ape of South Africa. In: Laura, Garwin, Tim, Lincoln (Eds.), A Century of Nature: Twenty-One Discoveries that Changed Science and the World, pp. 10–20.

De Schepper, S., Gibbard, P.L., Salzmann, U., Ehlers, J., 2014. A global synthesis of the marine and terrestrial evidence for glaciation during the Pliocene Epoch. Earth Sci. Rev. 135, 83–102.

Deino, A.L., Kingston, J.D., Glen, J.M., Edgar, R.K., Hill, A., 2006. Precessional forcing of lacustrine sedimentation in the late Cenozoic Chemeron Basin, Central Kenya Rift, and calibration of the Gauss/Matuyama boundary. Earth Planet. Sci. Lett. 247, 41–60.

Deino, A.L., Sier, M.J., Garello, D.I., Keller, B., Kingson, J.D., Scott, J.J., Dupont-Nivet, G., Cohen, A.S., this issue. Chronostratigraphy of the Baringo-Tugen-Barsemoi (HSPDP-BTB13-1A) core - 40Ar/39Ar dating, magnetostratigraphy, tephrostratigraphy, sequence stratigraphy and Bayesian age modeling. In Scott, J.J., Stone, J.R., Sier, M.J., Kingston, J.D. (eds.), A high-resolution, multi-proxy record of Pliocene hominin environments in the Kenya Rift Valley: Analysis of the Baringo-Tugen Hills-Barsemoi (BTB) Drill Core. Palaeogeography, Palaeoclimatology, Palaeoecology.

deMenocal, P.B., 1995. Plio-pleistocene african climate. Science 270, 53–59.

deMenocal, P.B., 2004. African climate change and faunal evolution during the Pliocene–Pleistocene. Earth Planet. Sci. Lett. 220, 3–24.

deMenocal, P.B., Ortiz, J., Guilderson, T., Adkins, J., Sarnthein, M., Baker, L., Yarusinsky, M., 2000. Abrupt onset and termination of the African Humid Period:: rapid climate responses to gradual insolation forcing. Quat. Sci. Rev. 19, 347–361.

Domínguez-Rodrigo, M., Barboni, D., Brugal, J.-P., Macho, G., Musiba, C.M., Pickering, T.R., Rook, L., White, T.D., Domínguez-Rodrigo, M., 2013. Savanna hypothesis, myth, and dilemma!. Curr. Anthropol. 55 000-000.

Eglinton, G., Hamilton, R.J., 1967. Leaf epicuticular waxes. Science 156, 1322–1335.

Eglinton, T.I., Eglinton, G., 2008. Molecular proxies for paleoclimatology. Earth Planet. Sci. Lett. 275, 1–16.

Feakins, S.J., 2013. Pollen-corrected leaf wax D/H reconstructions of northeast African hydrological changes during the late Miocene. Palaeogeogr. Palaeoclimatol. Palaeoecol. 374, 62–71.

Feakins, S.J., deMenocal, P.B., Eglinton, T.I., 2005. Biomarker records of late Neogene changes in northeast African vegetation. Geology 33, 977–980.

Feakins, S.J., Eglinton, T.I., 2007. A comparison of biomarker records of northeast African vegetation from lacustrine and marine sediments (ca. 3.40 Ma). Org. Geochem. 38, 1607–1624.

Feakins, S.J., Levin, N.E., Liddy, H.M., Sieracki, A., Eglinton, T.I., Bonnefille, R., 2013. Northeast African vegetation change over 12 my. Geology 41, 295–298.

Garcin, Y., Schwab, V.F., Gleixner, G., Kahmen, A., Todou, G., Séné, O., Onana, J.-M., Achoundong, G., Sachse, D., 2012. Hydrogen isotope ratios of lacustrine sedimentary n-alkanes as proxies of tropical African hydrology: insights from a calibration transect across Cameroon. Geochem. Cosmochim. Acta 79, 106–126.

Garello, D.I., Deino, A.L., Campisano, C.K., Kingston, J.D., this issue. Geochemical characterization of tephra from the upper Chemeron Formation (3.3-2.6 Ma), Baringo Basin, Kenya, and correlations between outcrop and the Baringo-Tugen Hills-Barsemoi drill core. In Scott, J.J., Stone, J.R., Sier, M.J., Kingston, J.D. (eds.), A high-resolution, multi-proxy record of Pliocene hominin environments in the Kenya Rift Valley: Analysis of the Baringo-Tugen Hills-Barsemoi (BTB) Drill Core. Palaeogeography, Palaeoclimatology, Palaeoecology, same special issue.

Grant, K.M., Rohling, E.J., Westerhold, T., Zabel, M., Heslop, D., Konijnendijk, T., Lourens, L., 2017. A 3 million year index for North African humidity/aridity and the implication of potential pan-African Humid periods. Quat. Sci. Rev. 171, 100–118.

Grove, M., 2014. Evolution and dispersal under climatic instability: a simple evolutionary algorithm. Adapt. Behav. 22, 235–254.

Grove, M., 2015. Palaeoclimates, plasticity, and the early dispersal of Homo sapiens. Quat. Int. 369, 17–37.

Hansen, M., DeFries, R., Townshend, J., Carroll, M., Dimiceli, C., Sohlberg, R., 2003. Global percent tree cover at a spatial resolution of 500 meters: first results of the MODIS vegetation continuous fields algorithm. Earth Interact. 7, 1–15.

Harmand, S., Lewis, J.E., Feibel, C.S., Lepre, C.J., Prat, S., Lenoble, A., Boës, X., Quinn, R.L., Brenet, M., Arroyo, A., 2015. 3.3-million-year-old stone tools from lomekwi 3, west Turkana, Kenya. Nature 521, 310–315.

Hatch, M.D., 1987. C4 photosynthesis: a unique elend of modified biochemistry, anatomy and ultrastructure. Biochim. Biophys. Acta 895, 81–106.

Hély, C., Bremond, L., Alleaume, S., Smith, B., Sykes, M.T., Guiot, J., 2006. Sensitivity of African biomes to changes in the precipitation regime. Glob. Ecol. Biogeogr. 15, 258–270.

Herbert, T.D., Peterson, L.C., Lawrence, K.T., Liu, Z., 2010. Tropical ocean temperatures over the past 3.5 million years. Science 328, 1530–1534.

Hill, A., 1985. Early hominid from Baringo, Kenya. Nature 315, 222.

Hill, A., Ward, S., 1988. Origin of the Hominidae: the record of African large hominoid evolution between 14 My and 4 My. Am. J. Phys. Anthropol. 31, 49–83.

Hill, A., Ward, S., Deino, A., Curtis, G., Drake, R., 1992. Earliest Homo. Nature 355, 719.

Ivory, S.J., Blome, M.W., King, J.W., McGlue, M.M., Cole, J.E., Cohen, A.S., 2016. Environmental change explains cichlid adaptive radiation at Lake Malawi over the past 1.2 million years. Proc. Natl. Acad. Sci. 113, 11895–11900.

Ivory, S.J., Lézine, A.-M., Vincens, A., Cohen, A.S., 2012. Effect of aridity and rainfall seasonality on vegetation in the southern tropics of East Africa during the

Pleistocene/Holocene transition. Quat. Res. 77, 77–86.
Ivory, S.J., Russell, J., 2016. Climate, herbivory, and fire controls on tropical African forest for the last 60ka. Quat. Sci. Rev. 148, 101–114.
Joordens, J.C., Vonhof, H.B., Feibel, C.S., Lourens, L.J., Dupont-Nivet, G., van der Lubbe, J.H., Sier, M.J., Davies, G.R., Kroon, D., 2011. An astronomically-tuned climate framework for hominins in the Turkana Basin. Earth Planet. Sci. Lett. 307, 1–8.
Kingston, J.D., 1999. Environmental determinants in early hominid evolution: issues and evidence from the Tugen Hills, Kenya. In: Late Cenozoic Environments and Hominid Evolution: a Tribute to Bill Bishop. Geological Society, London, pp. 69–84.
Kingston, J.D., Deino, A.L., Edgar, R.K., Hill, A., 2007. Astronomically forced climate change in the Kenyan Rift Valley 2.7–2.55 Ma: implications for the evolution of early hominin ecosystems. J. Hum. Evol. 53, 487–503.
Kingston, J.D., Hill, A., Marino, B.D., 1994. Isotopic evidence for neogene hominid paleoenvironments in the Kenya rift valley. Science 264, 955–959.
Kürschner, W.M., van der Burgh, J., Visscher, H., Dilcher, D.L., 1996. Oak leaves as biosensors of late Neogene and early Pleistocene paleoatmospheric CO2 concentrations. Mar. Micropaleontol. 27, 299–312.
Laskar, J., Robutel, P., Joutel, F., Gastineau, M., Correia, A., Levrard, B., 2004. A long-term numerical solution for the insolation quantities of the Earth. Astron. Astrophys. 428, 261–285.
Levin, N., 2013. Compilation of East Africa soil carbonate stable isotope data. Interdisciplinary Earth Data Alliance (IEDA). https://doi.org/10.1594/IEDA/100231.
Levin, N.E., 2015. Environment and climate of early human evolution. Annu. Rev. Earth Planet Sci. 43, 405–429.
Levin, N.E., Brown, F.H., Behrensmeyer, A.K., Bobe, R., Cerling, T.E., 2011. Paleosol carbonates from the Omo Group: isotopic records of local and regional environmental change in East Africa. Palaeogeogr. Palaeoclimatol. Palaeoecol. 307, 75–89.
Liddy, H.M., Feakins, S.J., Tierney, J.E., 2016. Cooling and drying in northeast Africa across the Pliocene. Earth Planet. Sci. Lett. 449, 430–438.
Lisiecki, L.E., Raymo, M.E., 2005. A Pliocene-Pleistocene stack of 57 globally distributed benthic δ18O records. Paleoceanography 20.
Lupien, R., Russell, J., Feibel, C., Beck, C., Castañeda, I., Deino, A., Cohen, A., 2018. A leaf wax biomarker record of early Pleistocene hydroclimate from West Turkana, Kenya. Quat. Sci. Rev. 186, 225–235.
Magill, C.R., Ashley, G.M., Freeman, K.H., 2013. Ecosystem variability and early human habitats in eastern Africa. Proc. Natl. Acad. Sci. 110, 1167–1174.
Maslin, M.A., Brierley, C.M., Milner, A.M., Shultz, S., Trauth, M.H., Wilson, K.E., 2014. East African climate pulses and early human evolution. Quat. Sci. Rev. 101, 1–17.
Maslin, M.A., Christensen, B., 2007. Tectonics, orbital forcing, global climate change, and human evolution in Africa: introduction to the African paleoclimate special volume. J. Hum. Evol. 53, 443–464.
Maslin, M.A., Trauth, M.H., 2009. Plio-Pleistocene East African Pulsed Climate Variability and its Influence on Early Human Evolution. Vertebrate Paleobiology and Paleoanthropology Series, pp. 151.
Meyers, P.A., 2003. Applications of organic geochemistry to paleolimnological reconstructions: a summary of examples from the Laurentian Great Lakes. Org. Geochem. 34, 261–289.
Meyers, P.A., Ishiwatari, R., 1993. Lacustrine organic geochemistry—an overview of indicators of organic matter sources and diagenesis in lake sediments. Org. Geochem. 20, 867–900.
Meyers, P.A., Lallier-Vergès, E., 1999. Lacustrine sedimentary organic matter records of Late Quaternary paleoclimates. J. Paleolimnol. 21, 345–372.
Minkara, K.E., Deocampo, D.M., Rabideaux, N.M., Kingston, J.D., Deino, A.L., Cohen, A. S., Campisano, C.J., this issue. Zeolite facies and implications for environmental change from the Chemeron Formation of the Baringo Basin, Kenya Rift, 3.3-2.6 Ma. In Scott, J.J., Stone, J.R., Sier, M.J., Kingston, J.D. (eds.), A high-resolution, multi-proxy record of Pliocene hominin environments in the Kenya Rift Valley: Analysis of the Baringo-Tugen Hills-Barsemoi (BTB) Drill Core. Palaeogeography, Palaeoclimatology, Palaeoecology.
Nutz, A., Schuster, M., Boës, X., Rubino, J.-L., 2017. Orbitally-driven evolution of lake Turkana (Turkana depression, Kenya, EARS) between 1.95 and 1.72 Ma: a sequence stratigraphy perspective. J. Afr. Earth Sci. 125, 230–243.
O'Leary, M.H., 1981. Carbon isotope fractionation in plants. Phytochemistry 20, 553–567.
Otto-Bliesner, B.L., Russell, J.M., Clark, P.U., Liu, Z., Overpeck, J.T., Konecky, B., Nicholson, S.E., He, F., Lu, Z., 2014. Coherent changes of southeastern equatorial and northern African rainfall during the last deglaciation. Science 346, 1223–1227.
Pagani, M., Liu, Z., LaRiviere, J., Ravelo, A.C., 2010. High Earth-system climate sensitivity determined from Pliocene carbon dioxide concentrations. Nat. Geosci. 3, 27–30.
Polissar, P.J., Rose, C., Uno, K.T., Phelps, S.R., deMenocal, P., 2019. Synchronous rise of African C4 ecosystems 10 million years ago in the absence of aridification. Nat. Geosci. 12, 657–660.
Potts, R., 1996. Evolution and climate variability. Science 273, 922.
Potts, R., 1998. Variability selection in hominid evolution. Evol. Anthropol. Issues News Rev. 7, 81–96.
Potts, R., 2013. Hominin evolution in settings of strong environmental variability. Quat. Sci. Rev. 73, 1–13.
Potts, R., Faith, J.T., 2015. Alternating high and low climate variability: the context of natural selection and speciation in Plio-Pleistocene hominin evolution. J. Hum. Evol. 87, 5–20.
Raymo, M., Grant, B., Horowitz, M., Rau, G., 1996. Mid-Pliocene warmth: stronger greenhouse and stronger conveyor. Mar. Micropaleontol. 27, 313–326.
Rose, C., Polissar, P.J., Tierney, J.E., Filley, T., deMenocal, P.B., 2016. Changes in northeast African hydrology and vegetation associated with Pliocene–Pleistocene sapropel cycles. In: Philosophical Transactions of the Royal Society of London B: Biological Sciences, vol. 371.
Rossie, J.B., Hill, A., 2018. A new species of simiolus from the middle Miocene of the tugen Hills, Kenya. J. Hum. Evol. 125, 50–58.
Rossignol-Strick, M., 1983. African monsoons, an immediate climate response to orbital insolation. Nature 304, 46–49.
Rossignol-Strick, M., 1985. Mediterranean Quaternary sapropels, an immediate response of the African monsoon to variation of insolation. Palaeogeogr. Palaeoclimatol. Palaeoecol. 49, 237–263.
Rozanski, K., Araguás-Araguás, L., Gonfiantini, R., 1993. Isotopic Patterns in Modern Global Precipitation.
Russell, J.M., McCoy, S., Verschuren, D., Bessems, I., Huang, Y., 2009. Human impacts, climate change, and aquatic ecosystem response during the past 2000 yr at Lake Wandakara, Uganda. Quat. Res. 72, 315–324.
Sachse, D., Billault, I., Bowen, G.J., Chikaraishi, Y., Dawson, T.E., Feakins, S.J., Freeman, K.H., Magill, C.R., McInerney, F.A., Van Der Meer, M.T., 2012. Molecular paleohydrology: interpreting the hydrogen-isotopic composition of lipid biomarkers from photosynthesizing organisms. Annu. Rev. Earth Planet Sci. 40, 221–249.
Sachse, D., Radke, J., Gleixner, G., 2004. Hydrogen isotope ratios of recent lacustrine sedimentary n-alkanes record modern climate variability. Geochem. Cosmochim. Acta 68, 4877–4889.
Scott, J.J., Chupik, D.T., Deino, A.L., Stockhecke, M., Kingston, J.D., Westover, K.S., Lukens, W.E., Deocampo, D.M., Yost, C.L., Billingsley, A.L., Minkara, K.E., Ortiz, K., Cohen, A.S., this issue. Sequence stratigraphic framework for lacustrine transgression-regression cycles in the 3.3-2.6 Ma interval of the Chemeron Formation BTB13 core, Baringo Basin, Kenya Rift Valley. In Scott, J.J., Stone, J.R., Sier, M.J., Kingston, J.D. (eds.), A high-resolution, multi-proxy record of Pliocene hominin environments in the Kenya Rift Valley: Analysis of the Baringo-Tugen Hills-Barsemoi (BTB) Drill Core. Palaeogeography, Palaeoclimatology, Palaeoecology.
Seki, O., Foster, G.L., Schmidt, D.N., Mackensen, A., Kawamura, K., Pancost, R.D., 2010. Alkenone and boron-based Pliocene pCO 2 records. Earth Planet. Sci. Lett. 292, 201–211.
Shanahan, T.M., McKay, N.P., Hughen, K.A., Overpeck, J.T., Otto-Bliesner, B., Heil, C.W., King, J., Scholz, C.A., Peck, J., 2015. The time-transgressive termination of the african Humid Period. Nat. Geosci. 8, 140–144.
Sherwood, R.J., Ward, S.C., Hill, A., 2002. The taxonomic status of the Chemeron temporal (KNM-BC 1). J. Hum. Evol. 42, 153–184.
Shultz, S., Nelson, E., Dunbar, R.I., 2012. Hominin cognitive evolution: identifying patterns and processes in the fossil and archaeological record. Philos. Trans. R. Soc. Lond. B Biol. Sci. 367, 2130–2140.
Sier, M.J., Dupont-Nivet, G., Langereis, C., Deino, A.L., Kingston, J.D., Cohen, A.S., 2019. this issue. Magnetostratigraphy of the Hominin Sites and Paleolakes Drilling Project (HSPDP) Baringo-Tugen Hills-Barsemoi core (Kenya). In Scott, J.J., Stone, J.R., Sier, M.J., Kingston, J.D. (eds.), A high-resolution, multi-proxy record of Pliocene hominin environments in the Kenya Rift Valley: Analysis of the Baringo-Tugen Hills-Barsemoi (BTB) Drill Core. Palaeogeography, Palaeoclimatology, Palaeoecology.
Talbot, M.R., Jensen, N.B., Lærdal, T., Filippi, M.L., 2006. Geochemical responses to a major transgression in giant African lakes. J. Paleolimnol. 35, 467–489.
Tierney, J.E., deMenocal, P., Zander, P.D., 2017. A climatic context for the out-of-Africa migration. Geology 45, 1023–1026.
Tobias, P.V., 1995. The brain of the first hominids. Orig. Hum. Brain 61–83.
Trauth, M.H., Maslin, M.A., Deino, A., Strecker, M.R., 2005. Late Cenozoic moisture history of East Africa. Science 309, 2051–2053.
Trauth, M.H., Maslin, M.A., Deino, A.L., Junginger, A., Lesoloyia, M., Odada, E.O., Olago, D.O., Olaka, L.A., Strecker, M.R., Tiedemann, R., 2010. Human evolution in a variable environment: the amplifier lakes of Eastern Africa. Quat. Sci. Rev. 29, 2981–2988.
Trauth, M.H., Maslin, M.A., Deino, A.L., Strecker, M.R., Bergner, A.G., Dühnforth, M., 2007. High-and low-latitude forcing of Plio-Pleistocene East African climate and human evolution. J. Hum. Evol. 53, 475–486.
Tripati, A.K., Roberts, C.D., Eagle, R.A., 2009. Coupling of CO_2 and ice sheet stability over major climate transitions of the last 20 million years. Science 326, 1394–1397.
Uno, K.T., Polissar, P.J., Jackson, K.E., deMenocal, P.B., 2016a. Neogene biomarker record of vegetation change in eastern Africa. In: Proceedings of the National Academy of Sciences.
Uno, K.T., Polissar, P.J., Kahle, E., Feibel, C., Harmand, S., Roche, H., deMenocal, P.B., 2016b. A Pleistocene palaeovegetation record from plant wax biomarkers from the Nachukui Formation, West Turkana, Kenya. In: Philosophical Transactions of the Royal Society of London B: Biological Sciences, vol. 371.
Villmoare, B., Kimbel, W.H., Seyoum, C., Campisano, C.J., DiMaggio, E.N., Rowan, J., Braun, D.R., Arrowsmith, J.R., Reed, K.E., 2015. Early Homo at 2.8 Ma from Ledi-Geraru, Afar, Ethiopia. Science 347, 1352–1355.
Vogts, A., Moossen, H., Rommerskirchen, F., Rullkötter, J., 2009. Distribution patterns and stable carbon isotopic composition of alkanes and alkan-1-ols from plant waxes of African rain forest and savanna C 3 species. Org. Geochem. 40, 1037–1054.
Volkman, J.K., Barrett, S.M., Blackburn, S.I., Mansour, M.P., Sikes, E.L., Gelin, F., 1998. Microalgal biomarkers: a review of recent research developments. Org. Geochem. 29, 1163–1179.
Vrba, E.S., 1985. Environment and evolution: alternative causes of the temporal distribution of evolutionary events. South Afr. J. Sci. 81, 229–236.
Vrba, E.S., 1993. Turnover-pulses, the red queen, and related topics. Am. J. Sci. 293, 418–452.
Vrba, E.S., 1995. On the connections between paleoclimate and evolution. In: Vrba, E.S., Denton, G.H., Partridge, T.C., Burckle, L.H. (Eds.), Paleoclimate and Evolution with Emphasis on Human Origins, pp. 24–45.
Ward, S., Brown, B., Hill, A., Kelley, J., Downs, W., 1999. Equatorius: a new hominoid genus from the middle Miocene of Kenya. Science 285, 1382–1386.

Webb, M., Barker, P.A., Wynn, P.M., Heiri, O., Van Hardenbroek, M., Pick, F., Russell, J.M., Stott, A.W., Leng, M.J., 2016. Interpretation and application of carbon isotope ratios in freshwater diatom silica. J. Quat. Sci. 31, 300–309.

Westover, K.S., Stone, J.R., Yost, C.L., Scott, J.J., Cohen, A.S., Rabideaux, N.M., Stockhecke, M., Kingston, J.D., this issue. Diatom paleolimnology of late Pliocene Baringo Basin (Kenya) paleolakes. In Scott, J.J., Stone, J.R., Sier, M.J., Kingston, J.D. (eds.), A high-resolution, multi-proxy record of Pliocene hominin environments in the Kenya Rift Valley: Analysis of the Baringo-Tugen Hills-Barsemoi (BTB) Drill Core. Palaeogeography, Palaeoclimatology, Palaeoecology.

White, F., 1983. The Vegetation of Africa: a Descriptive Memoir to Accompany the UNESCO/AETFAT/UNSO Vegetation Map of Africa by F White. Natural Resources Research Report XX. UNESCO, Paris, France.

Yost, C.L., Ivory, S.J., Deino, A.L., Rabideaux, N.M., Kingston, J.D., Cohen, A.S., this issue. Phytoliths, pollen, and microcharcoal from the Baringo Basin, Kenya reveal savanna dynamics during the Plio-Pleistocene transition. In Scott, J.J., Stone, J.R., Sier, M.J., Kingston, J.D. (eds.), A high-resolution, multi-proxy record of Pliocene hominin environments in the Kenya Rift Valley: Analysis of the Baringo-Tugen Hills-Barsemoi (BTB) Drill Core. Palaeogeography, Palaeoclimatology, Palaeoecology.

Yost, C.L., Jackson, L.J., Stone, J.R., Cohen, A.S., 2018. Subdecadal phytolith and charcoal records from Lake Malawi, East Africa imply minimal effects on human evolution from the~ 74 ka Toba supereruption. J. Hum. Evol. 116, 75–94.

Zachos, J., Pagani, M., Sloan, L., Thomas, E., Billups, K., 2001. Trends, rhythms, and aberrations in global climate 65 Ma to present. Science 292, 686–693.